

*Proceedings of the Korean Nuclear Society Spring Meeting*  
*Kori, Korea, May 2000*

## **Development and verification of a corrosion model by using a high burnup database**

Byung Ho LEE, Yang Hyun KOO, and Dong Seong SOHN  
Korea Atomic Energy Research Institute

Nadeem Elahi  
Pakistan Atomic Energy Commission

### **ABSTRACT**

A semi-empirical corrosion model for Zircaloy-4 cladding for PWRs has been developed by focusing particularly on the metallurgical effect and the Sn content in the cladding composition. The Sn effect on corrosion is estimated by analyzing the measured corrosion data, which shows a linear increase with Sn content. Concerning the metallurgical effect, the corrosion behavior shows a Gaussian dependency on precipitate size that is determined by the accumulated annealing parameter.

The model is incorporated in a fuel rod performance code, COSMOS, and used to calculate the corrosion thickness over a wide range of available data, which covers the particular corrosion behavior for irradiation history and condition, and the manufacturing history of the cladding. The predicted oxide thickness values lie within the error boundary of  $\pm 20 \mu\text{m}$ , compared to the measured ones.

The present model shows that the effects of both metallurgy and Sn content should be included to analyze the corrosion behavior of Zircaloy-4 cladding irradiated at high burnups.

## 1. INTRODUCTION

Corrosion of Zircaloy cladding in PWRs has become more important due to

- higher fuel discharge burnup to reduce fuel cycle costs,
- higher coolant inlet temperature to increase plant thermal efficiency, and
- the increase of coolant pH and lithium concentration to reduce plant radiation levels.

The corrosion kinetics for Zircaloy-4 falls into two periods referred as pre- and post-transition. The initial, pre-transition period is characterized by a decreasing corrosion rate, which shows the almost cubic growth of oxide. When the oxide reaches a thickness of about 2  $\mu\text{m}$  (the transition point), the oxidation rate increases at an approximately linear rate. The oxide layer during the pre-transition has a very compact and protective *tetragonal* structure, and a black and lustrous color, whereas the oxide after pre-transition has a friable and gray *monoclinic* structure.

The corrosion behavior of Zircaloy-4 depends upon a number of factors. One of the most significant factors that influence the corrosion of Zircaloy-4 is Sn composition of the Zircaloy-4 alloying element. Since the 1980s a tin content of 1.5 ~ 1.6 wt. % in the former “Standard” Zircaloy-4 cladding was added to increase corrosion resistance, especially to mitigate the deleterious effect of nitrogen deteriorating the corrosion resistance. Due to the improved control of processing parameters, and consequently of nitrogen content, it is now possible to reduce the tin content, if desired. Lowering the tin content reduces the solubility of iron hence reducing the uniform oxide growth rate. Thus, Sn content has been lowered to 1.2 ~ 1.4 wt% for the present “Improved” or low Sn Zircaloy-4 cladding.

The primary metallurgical factors that have been found to correlate with the corrosion resistance of Zircaloy are the size and distribution of the second phase particles. The alloying elements such as Fe, Cr and Ni have less solubility in  $\alpha$  Zirconium. Therefore, the major fractions of these alloying elements are always present at operational temperatures in the form of precipitates. It has been established that particle size and distribution depend on the details of the cladding after  $\beta$ -phase homogenization including the annealing temperatures and the time after cold working to a specified tube dimension.

Keeping this in mind, a semi-empirical corrosion model for Zircaloy–4 cladding was developed to take account into the tin content in the cladding alloy, as well as the metallurgical variables of the cladding. The developed model, after the incorporation into KAERI’s fuel performance code, COSMOS [1], was verified by forty five measured cladding oxide thickness data from UO<sub>2</sub> fuel rods irradiated in different PWRs [2].

## 2. DESCRIPTION of SEMI- EMPIRICAL CORROSION MODEL

As one of the perpetual efforts to increase fuel reliability, a phenomenological corrosion model for Zircaloy–4 cladding in PWRs has been developed and implemented in the fuel performance code, COSMOS [1]. The developed model focuses to take tin content in the cladding composition into account, as well as the accumulative annealing parameter effects on the corrosion of Zircaloy–4.

The oxidation process of Zircaloy cladding can be estimated using semi–empirical correlations divided by pre–transition and post–transition kinetics. The Zircaloy corrosion process is essentially a diffusion–controlled reaction; Zircaloy oxidation kinetics are presented by the Arrhenius equation as a function of temperature, activation energy, and additional acceleration factors.

In general, the corrosion rate equation in the pre–transition regime is given by

$$\frac{d\mathbf{d}^3}{dt} = K_{pre} \cdot \exp\left(-\frac{Q_{pre}}{R \cdot T_i}\right) \quad (\text{mm}^3/\text{day})$$

$$K_{pre} = F_{Sn} \cdot F_A \cdot F_{Li} \cdot F_{pre}$$

while the oxidation rate in the post–transition regime is given by

$$\frac{d\mathbf{d}}{dt} = K_{post} \cdot \exp\left(-\frac{Q_{post}}{R \cdot T_i}\right) \quad (\text{mm}/\text{day})$$

$$K_{post} = F_{Sn} \cdot F_A \cdot F_{Li} \cdot F_f \cdot F_{post}$$

$$F_f = C_1 + C_2 \cdot (C_3 \cdot \mathbf{f})^{C_4}$$

where

- $d$  = oxidation thickness [mm]
- $R$  = universal gas constant = 1.986 [cal/mol–K]
- $T_i$  = metal/oxide interface temperature [K]
- $K_{pre}$  = frequency factor for pre–transition regime [mm<sup>3</sup>/day]
- $K_{post}$  = frequency factor for post–transition regime [mm/day]
- $Q_{pre}$  = activation energy for pre transition = 32,269 [cal/mol–K]
- $Q_{post}$  = activation energy for post transition = 27,150 [cal/mol–K]
- $F_{Sn}$  = corrosion enhancement factor as function of Sn content
- $F_A$  = corrosion enhancement factor as function of accumulative annealing parameter
- $F_{Li}$  = corrosion enhancement factor by lithium concentration in the coolant
- $F_f$  = fast neutron flux enhancement factor
- $\phi$  = fast neutron flux (> 0.821 MeV) [n/cm<sup>2</sup>–s]
- $C_1, C_2, C_3, C_4$  = constants to determine the irradiation enhancement factor.

Among the many factors in the Zircaloy corrosion model, we only improved the following acceleration effects:

- Tin content in Zircaloy composition
- Accumulated annealing parameter

The differential equation of oxide thickness is solved numerically by a fourth order Runge–Kutta integration formulae [3].

## 2.1 Tin Effect

A significant improvement in standard Zircaloy-4 cladding performance was obtained by a reduction in the tin concentration, within the ASTM specified ranges. This development was

initiated by a statistical evaluation of the corrosion behavior of standard Zircaloy-4 in different PWRs, which revealed that variations in the alloy chemistry were one of the factors responsible for the observed scatter. To clarify the alloying, especially, the Sn effect on corrosion behavior, low tin Zircaloy-4 with Sn levels typically between 1.2% and 1.4% was irradiated to more than 50 MWd/kgU burnup in a high temperature PWR plant. As expected, the corrosion rate of the low Sn Zircaloy-4 was near the lower range of the band observed for ASTM specified Zircaloy-4. Under normal operating conditions, standard Zircaloy-4 cladding will reach an oxide thickness of 100  $\mu\text{m}$  at a burnup of 45 ~ 55 MWd/kgU, while improved low tin Zircaloy-4 may reach that value at a higher burnup range of 50 ~ 60 MWd/kgU or higher [4].

Fig. 1 shows the in-pile relative corrosion rate as a function of Sn content.

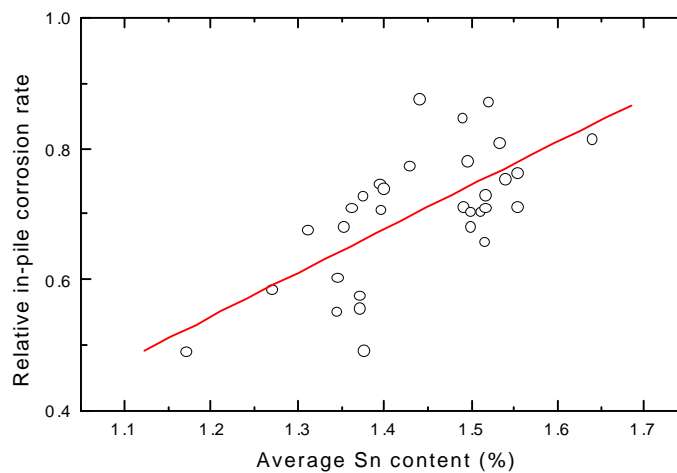


Fig. 1 Relative in-pile corrosion rate as a function of Sn content.

The least-squares method using a linear relationship yields the following formula for the Sn effect,  $F_{Sn}$ , on corrosion behavior:

$$F_{Sn} = -0.2557 + 0.6666 \times SN$$

where SN is the concentration of tin in the Zircaloy-4 cladding.

This Sn factor is included in the frequency factor as a multiplicative coefficient.

## 2.2 Annealing Effect

Precipitate size and the accumulated annealing parameter have a significant effect on corrosion behavior. The accumulated annealing parameter sums up all applied heat temperatures in the  $\alpha$ -phase region of zirconium during fabrication:

$$\Sigma A_i = \Sigma \left[ t_i \cdot \exp \left( -\frac{Q}{R \cdot T_i} \right) \right]$$

where the activation energy  $Q/R \cong 40,000$  K, and  $t_i$  is the effective time of annealing step  $i$ , at temperature  $T_i$ . This parameter is termed as the annealing parameter,  $A$ .

There is a clear correlation between the size of the intermetallic precipitates and the applied annealing conditions expressed by the accumulated annealing parameter [5]. Fig. 2 correlates the determined mean particle size of the intermetallic precipitates in Zircaloy-4 with the accumulated annealing parameter  $\Sigma A_i$ , using an activation temperature  $Q/R$  of 40,000 K.

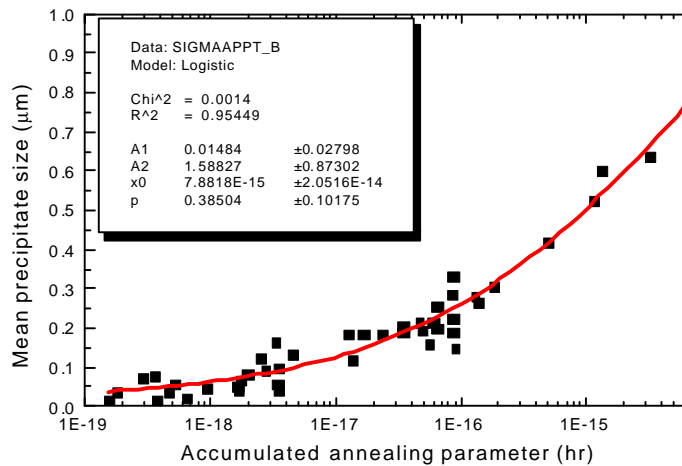


Fig. 2 Intermetallic precipitate size as a function of the accumulated annealing parameter.

This figure shows that the increase of particle size starts at the  $\Sigma A_i$  value of  $10^{-18}$  h. Note that this correlation is independent of the number and sequence of the annealing in the  $\alpha$ -range and is not affected by the intermediate cold-working steps.

By fitting the measured data with sigmoidal analysis using a Logistical equation, the mean particle size gives the following results:

$$MPS = 1.58827 - \frac{1.573}{1.0 + \left( \frac{\sum A_i}{7.8818 \times 10^{-15}} \right)^{0.38504}}$$

where MPS is the mean precipitate size in  $\mu\text{m}$ .

From the knowledge of the reported values of the annealing parameter, this correlation can be used to determine the mean size of the intermetallic precipitates in Zircaloy-4.

Fig. 3 shows the dependence of the corrosion rate on the average precipitate diameter, which can be determined from the above equation.

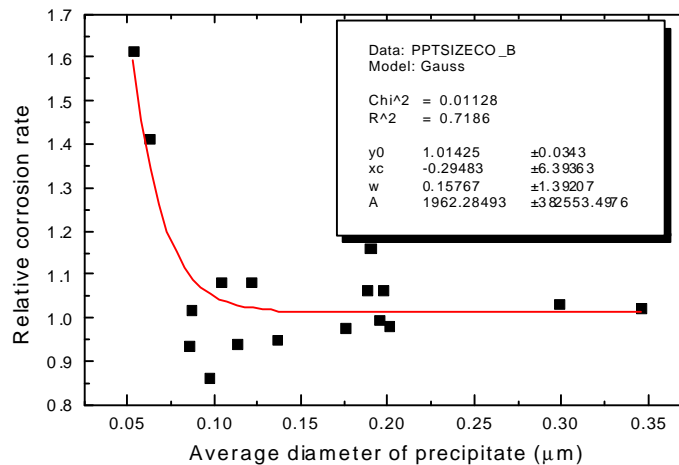


Fig. 3 Relative corrosion rate as a function of intermetallic precipitate size.

The measured data are curve-fitted by a Gaussian relationship such as

$$F_{MPS} = 1.01425 + 9932.58 \cdot \exp\left(-2 \cdot \left(\frac{MPS + 0.29483}{0.15767}\right)^2\right)$$

From this derived relationship, the metallurgical effect of Zircaloy-4 on corrosion behavior can be described.

### 3. VERIFICATION OF THE DEVELOPED MODEL

The developed corrosion model was verified by the corrosion database obtained by the measured data [2], which is composed of (1) the irradiation history and condition, (2) the cladding properties, and (3) the measured oxide thickness. The summary for the database is listed in Table 1.

Table 1 Population and Characteristics of the Reactors

<b>Plant</b>	<b>Population</b>	<b>Distinguished characteristics</b>
A	6	High temperature PWR, high tin content rods
B	16	High time integrated LiOH exposure
C	5	Medium tin content rods
D	12	High as well as low tin content rods
E	6	High temperature PWR, different intermetallic particle size distribution.

Plant A is characterized by its high coolant temperature and high tin content. Six rods of this plant were irradiated. As shown in Fig. 4, the typically predicted oxide thickness was slightly higher than the measured one for these rods. The predicted corrosion thicknesses of rods 1, 2 and 3 were comparable to the measured results. For rods 5 and 6, where the thermo-hydraulic parameters were different, the predicted values were much greater than the measured ones. Rod 4 was purposely manufactured with a low tin content. The predicted corrosion thickness of rod 4 is in very good agreement with the measured results.

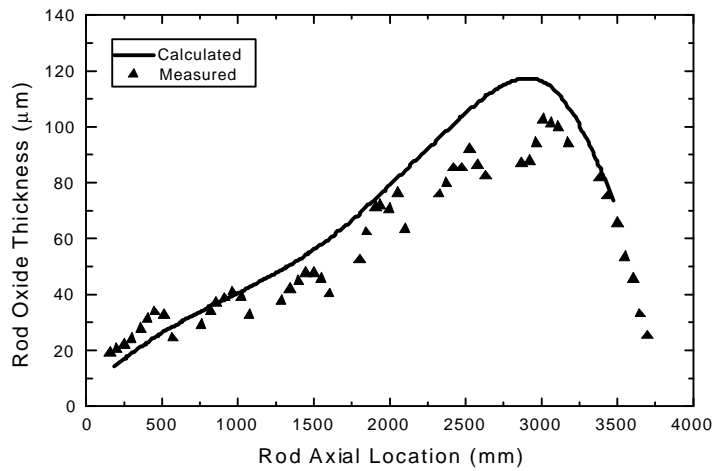


Fig. 4 Oxide thickness for Rod 1 of Plant A at EOL.

Plant B was of interest due to its high LiOH exposure. The predicted values of corrosion thickness are very close to that of the measured values for most of the cases throughout the length of the rods. In some cases, such as rods 1 and 5, there is a sharp increase in the measured oxide thickness at the peak oxide position. In these cases the peak measured oxide thicknesses are higher than the predicted values. For the low burnup rods 13, 15 and 16, where the measured oxide thicknesses are low, the developed model over-estimated the oxide thickness. Initially it was thought that a high LiOH content history may result in a high corrosion rate, but later it was not confirmed by the experimental investigation. This indiscernible lithium effect on corrosion behavior is caused by the negligible void in the coolant, at which the low linear heat generation rate cannot form the necessary void to concentrate lithium on the cladding surface [6].

The Zr-4 cladding used for the plant C rods is of medium tin content. A relatively large difference is observed between the predicted and measured oxide profiles of rods 1, 2 and 3. The thermo-hydraulic parameters are different for rods 4 and 5, due to the change of rod location. For rod 4 the predicted oxide thickness is higher than the measured values, particularly at the peak oxide location. In the case of rod 5, an excellent match exists between the predicted and measured oxide profile.

There are twelve rods pertaining to plant D. The tin content for these rods is both high and low. The predicted profiles for these rods are, in general, lower than the measured ones. However, the difference is about 20 $\mu\text{m}$  for rods 1 to 6. Although the low predicted results of rods 7, 8, 9 and 11 are quite comparable to the measured results, the predicted profiles for rod 10 and 12 are very close to that of measured values.

The distinguishing characteristic of the Plant E rods is that different precipitate sizes were intentionally used to verify the effect of intermetallic precipitates on the corrosion of Zr-4. The predicted behavior of plant E rods is similar to those of Plant D. Although predicted corrosion thickness is comparable to that of measured corrosion, it is generally low for rods 1~4, whereas for rods 5 and 6 the results are in good agreement with measured results.

It is observed during analysis that the maximum difference of measured and predicted oxide thickness is found at peak oxide thickness. Peak oxide thickness versus measured for all 45 rods was plotted with a 20 $\mu\text{m}$  error band as shown in Fig. 5. It can be concluded that the majority of the data points lie in the error band or close to it.

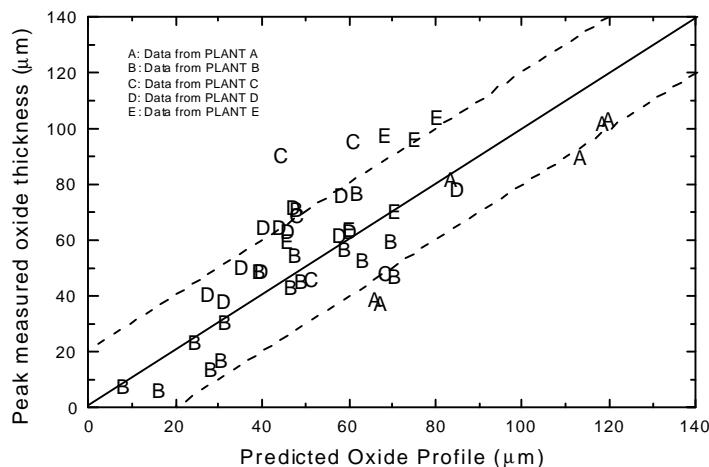


Fig. 5 Peak measured vs. predicted oxide thickness.

## 4. CONCLUSION

A semi-empirical corrosion model for Zircaloy-4 cladding for PWRs was developed to take into account the metallurgical effect as well as the tin contents in the cladding composition.

The Sn effect is estimated by analyzing the measured corrosion data, which shows a linear increase with Sn contents. Concerning the metallurgical effect, the corrosion behavior shows a sigmoidal dependency on the precipitate size, which is determined by the accumulated annealing parameter. The in-pile corrosion rate decreases with precipitate size and then stabilizes after the average precipitate size reaches 0.1  $\mu\text{m}$ .

The model is incorporated in a fuel rod performance code, COSMOS, and used to calculate corrosion thickness over a wide range of available data. The predicted oxide thickness values lie in the error boundary of  $\pm 20$   $\mu\text{m}$  in comparison to the measured ones.

Agreement between predicted oxide thicknesses with the measured data shows the good ability of the present model to estimate cladding oxidation.

### Acknowledgements

The authors would like to express their appreciation to the Ministry of Science and Technology (MOST) of the Republic of Korea for the support of this work through the mid- and long-term nuclear R&D Project.

### REFERENCES

- [1] Yang-Hyun Koo, Byung-Ho Lee, Dong-Seong Sohn, "COSMOS : A Computer Code for the analysis of LWR  $\text{UO}_2$  and MOX Fuel Rod," Journal of Korean Nuclear Society, 30 (1999) 541-554.
- [2] P.M. Gilmore, J.C. Gillis, H.H. Klepfer, and J.M. Sorensen, "EPRI PWR fuel cladding corrosion (PFCC) model, volume 2: corrosion theory and rate equation development," EPRI TR-105387-V2, 1996.

- [3] W.H. Press, B.P. Flannery, S.A. Teukolsky, and W.T. Betterling, "Numerical recipes," Cambridge university press (1986).
- [4] Garzarolli, G., Steingerg, E., Weidinger, H.G., "Microstructure and corrosion studies for optimized PWR and BWR Zircaloy cladding," Zirconium in the Nuclear Industry: 8<sup>th</sup> Int. Symp., ASTM STP-1023, L. F. P. Van Swam and C. M. Eucken, Eds, American Society for Testing and Materials, Philadelphia, (1988) 202-212.
- [5] Garzarolli, F., Stehle, H., "Behavior of structural materials for fuel and control elements in light water cooled power reactors," IAEA STI/PUB/721, International Atomic Energy Agency, Vienna, (1987) p 387.
- [6] B.H.Lee, Y.H.Koo, D.S.Sohn, "Void effect combined with water chemistry on corrosion behavior of Zircaloy-4 cladding in PWR," ANS topical meeting, Park city, USA, 2000.